Journal of Quantitative Spectroscopy & Radiative Transfer ▮ (▮▮▮▮) ▮▮▮–▮▮▮

Contents lists available at ScienceDirect

Journal of Quantitative Spectroscopy & Radiative Transfer

journal homepage: www.elsevier.com/locate/jqsrt

Canopy spectral invariants. Part 1: A new concept in remote sensing of vegetation

Yuri Knyazikhin*, Mitchell A. Schull, Liang Xu, Ranga B. Myneni, Arindam Samanta

Department of Geography and Environment, Boston University, 675 Commonwealth Avenue, Boston, MA 02215, USA

ARTICLE INFO

Keywords:
MODIS
MISR
Scale
Canopy structure
Canopy spectral invariants
Radiative transfer equation
Eigenvalues
Eigenvectors

ABSTRACT

The concept of canopy spectral invariants expresses the observation that simple algebraic combinations of leaf and canopy spectral reflectance become wavelength independent and determine two canopy structure specific variables – the recollision and escape probabilities. These variables specify an accurate relationship between the spectral response of a vegetation canopy to incident solar radiation at the leaf and the canopy scale. They are sensitive to important structural features of the canopy such as forest cover, tree density, leaf area index, crown geometry, forest type and stand age. This paper presents the mathematical basis of the concept which is linked to eigenvalues and eigenvectors of the three-dimensional radiative transfer equation.

1. Introduction

Interaction of solar radiation with the vegetation canopy is described by the three-dimensional radiative transfer equation [1,2]. The interaction cross-section that appears in this equation is treated as wavelength independent considering the size of the scattering elements (leaves, branches, twigs, etc.) relative to the wavelength of solar radiation [1]. Although the scattering and absorption processes are different at different wavelengths, the interaction probabilities for photons in vegetation media are determined by the structure of the canopy rather than photon frequency or the optics of the canopy. This feature results in unique spectrally invariant behavior for a vegetation canopy bounded from below by a non-reflecting surface: some simple algebraic combinations of the single-scattering albedo and canopy spectral transmittances and reflectances eliminate their dependencies on wavelength through the specification of two canopy structure specific spectrally invariant variables – the recollision and escape probabilities.

The recollision probability is the probability that a photon scattered from a phytoelement will interact within the canopy again [3] and is related to the maximum eigenvalue of the radiative transfer equation [4,5]. The escape probability is the probability that a scattered photon will escape the vegetation in a given direction [6]. These variables specify an accurate relationship between the spectral response of a vegetation canopy to the incident solar radiation at the leaf and the canopy scale and allows for a simple and accurate parameterization for the partitioning of the incoming radiation into canopy transmission, reflection and absorption at any wavelength in the solar spectrum. This result is essential to both modeling and remote sensing communities as it allows for the separation of the structural and radiometric components of the measured and/or modeled signal. The former is a function of canopy age, density and arrangement while the latter is a function of canopy biochemical behavior. Consequently, the canopy spectral invariants offer a simple and accurate parameterization of the shortwave radiation block in many global models of climate, hydrology, biogeochemistry, and ecology [7,8].

In remote sensing applications, the information content of spectral data can be fully exploited if the wavelength independent variables can be retrieved, for

* Corresponding author. Tel.: +1 617 353 8843; fax: +1 617 353 8846.
E-mail address: jknjazi@bu.edu (Y. Knyazikhin).

0022-4073/$ - see front matter © 2010 Elsevier Ltd. All rights reserved.
doi:10.1016/j.jqsrt.2010.06.014

they can be more directly related to structural characteristics of the vegetation canopy. This concept underlies the operational algorithm of global leaf area index, and the fraction of photosynthetically active radiation absorbed by vegetation developed for the moderate resolution imaging spectroradiometer (MODIS) and multi-angle imaging spectroradiometer (MISR) instruments of the Earth observing system (EOS) Terra mission [4,5]. The canopy spectral invariants have also been exploited in developing a 26 year leaf area index data record from multiple sensors [9,10]. Here we will discuss the theoretical basis of the concept and its potential utility for investigating the three-dimensional canopy structure from space measurements. In Part 2 [22], we will apply the concept to the classification of forest types from hyperspectral data.

2. Radiative transfer in vegetation canopies

Let $V\subset R^3$ and δV be the domain where radiative transfer occurs and its boundary, respectively. The domain V can be a shoot, tree crown, or a part of the vegetation canopy with several trees, etc. In remote sensing, V is a parallelepiped of horizontal dimensions X, Y and biome dependent height Z and represents a pixel in which a vegetation canopy is located [2,5]. The function characterizing the radiative field in V is the monochromatic intensity $I_\lambda(\boldsymbol{x},\Omega)$ depending on wavelength, λ, location $\boldsymbol{x}$ and direction Ω. Assuming no polarization and emission within the canopy, the monochromatic intensity distribution function is given by the boundary value problem for steady-state radiative transfer equation [1,2]:

$$LI_\lambda = S_\lambda I_\lambda, \tag{1}$$

$$I_\lambda(\mathbf{x}_B,\Omega) = \pi^{-1}\int_{\mathbf{n}_B\cdot\Omega'>0}\rho_\lambda(\mathbf{x}_B,\Omega',\Omega)I_\lambda(\mathbf{x}_B,\Omega')\left|\mathbf{n}_B\cdot\Omega'\right|d\Omega' + q_\lambda(\mathbf{x}_B,\Omega),$$
$$\mathbf{n}_B\cdot\Omega<0,\quad \mathbf{x}_B\in\delta V. \tag{2}$$

Here L and S_λ are the streaming-collision and scattering linear operators defined as

$$LI_\lambda = \frac{1}{\sigma(\boldsymbol{x},\Omega)}\Omega\cdot\nabla I_\lambda(\boldsymbol{x},\Omega) + I_\lambda(\boldsymbol{x},\Omega),$$
$$S_\lambda I_\lambda = \frac{1}{\sigma(\boldsymbol{x},\Omega)}\int_{4\pi}\sigma_{s,\lambda}(\boldsymbol{x},\Omega'\to\Omega)I_\lambda(\boldsymbol{x},\Omega')d\Omega'.$$

The term ρ_λ is the bidirectional reflectance factor of the boundary δV, q_λ describes the radiation penetrating into V through the boundary δV, $\mathbf{n}_B$ is the outward normal at $\mathbf{x}_B\in\delta V$, and 4π denotes the unit sphere. The boundary source q_λ at points $\boldsymbol{x}_T$ on the canopy top boundary is usually given by a mono-directional beam attenuated by the atmosphere, $c_\lambda\delta(\Omega-\Omega_0)$, and radiation scattered by the atmosphere $d_\lambda(\mathbf{x}_T,\Omega)$ (diffuse radiation), i.e., $q_\lambda(\mathbf{x}_T,\Omega) = c_\lambda\delta(\Omega-\Omega_0) + d_\lambda(x_T,\Omega)$, $\mathbf{n}_T\cdot\Omega<0$.

The interaction cross-section, σ, and differential cross-section, $\sigma_{s,\lambda}$, are defined as [1,2]:

$$\sigma(\mathbf{x},\Omega) = u_L(\boldsymbol{x})G(\mathbf{x},\Omega), \sigma_{s,\lambda}(\boldsymbol{x},\Omega'\to\Omega)$$
$$= u_L(\boldsymbol{x})\frac{1}{\pi}\Gamma_\lambda(\boldsymbol{x},\Omega'\to\Omega)$$

where $u_L(\boldsymbol{x})$ is the one-sided leaf area density distribution (in m^2/m^3), G is the geometry factor (dimensionless), and Γ_λ/π is the area scattering phase function (in sr^{-1}). The interaction cross-section is assumed to be strictly positive, i.e., $\sigma(\boldsymbol{x},\Omega)\geq\overline{\sigma}>0$. This inequality is required to apply mathematical techniques developed by Vladimirov [11], which will be used in Sections 3 and 4. It should be noted however that this condition can be released [12]. We also assume that $\Gamma_{s,\lambda}(\boldsymbol{x},\Omega'\to\Omega) = \Gamma_{s,\lambda}(\boldsymbol{x},-\Omega\to-\Omega') = \Gamma_{s,\lambda}(\boldsymbol{x},\Omega\to\Omega')$. These symmetry properties provide sufficient conditions for the validity of the reciprocity principle [13].

Note that the interaction cross-section is a function of the direction of photon travel. Also, the differential scattering cross-section is not, as a rule, rotationally invariant, i.e., it generally depends on the absolute directions of photon travel Ω' and Ω, before and after scattering, respectively, and not just the scattering angle $\cos^{-1}(\Omega'\cdot\Omega)$. These properties make solving of the radiative transfer equation more complicated; for example, the expansion of the differential scattering cross-section in spherical harmonics cannot be used. In contrast to radiative transfer in atmosphere the interaction cross-section in vegetation canopies is wavelength independent. This spectral invariance results in various unique relationships, which, to some degree, compensate for difficulties in solving the radiative transfer equation due to the above-mentioned features of the extinction and the differential scattering cross sections.

The interaction and differential cross sections are related as

$$\int_{4\pi}\sigma_{s,\lambda}(\boldsymbol{x},\Omega'\to\Omega)d\Omega = \omega(\lambda,\boldsymbol{x},\Omega')\sigma(\boldsymbol{x},\Omega')$$

where ω is the single scattering albedo. For ease of analysis, we assume that the single scattering albedo does not depend on $\boldsymbol{x}$ and Ω'. It coincides with the leaf albedo in this case. In the vegetation canopy angular distribution of radiation scattered by an elementary volume is mainly determined by geometrical properties of phytoelements resident in the volume [1,2]. Therefore we assume that the differential cross-section normalized by the single scattering albedo does not depend on wavelength. The scattering operator rearranges to $S_\lambda=\omega(\lambda)S_0$.

The three-dimensional radiative transfer problem with arbitrary boundary conditions can be expressed as a superposition of the solutions of some basic radiative transfer sub-problems with purely absorbing boundaries [13]. Therefore we restrict our consideration to the case when $\rho_\lambda=0$. We also assume that the source function q_λ does not depend on wavelength, $q_\lambda=q_0$. In optical remote sensing, the incident solar radiation is proportional to a wavelength dependent scalar. The latter condition therefore can be met by normalizing the boundary value problem by this scalar. Under the conditions discussed in this section, the single scattering albedo $\omega(\lambda)$ is the only variable that imbues wavelength dependency to the solution of the radiative transfer equation in vegetation canopies.

The formulation of radiative transfer presented here underlies the retrieval technique for producing global leaf area index and fraction of photosynthetically active

Please cite this article as: Knyazikhin Y, et al. Canopy spectral invariants. Part 1: A new concept in remote sensing of vegetation. JQSRT (2010), doi:10.1016/j.jqsrt.2010.06.014

radiation absorbed by vegetation from MODIS and MISR bidirectional reflectance factor (BRF) data products [4,5]. The BRF describes surface radiative response to mono-directional incident beam $c_\lambda\delta(\Omega-\Omega_0)$. The canopy BRF is the ratio of the radiance leaving the top of the vegetation canopy, $I_\lambda(\mathbf{x}_T,\Omega)$, to radiance, $(\pi)^{-1}c_\lambda|\mathbf{n}_T\cdot\Omega_0|$ reflected from an ideal Lambertian target into the same beam geometry and illuminated by the same mono-directional beam, i.e., $\mathrm{BRF}(\lambda,\Omega)=\pi I_\lambda(\mathbf{x}_T,\Omega)/|c_\lambda\mathbf{n}_T\cdot\Omega_0|$, $\mathbf{n}_T\cdot\Omega>0$, [14]. The dimensionless leaf area index (LAI) is defined as one-sided leaf area per unit ground area, i.e.,

$$\mathrm{LAI}=\frac{1}{X\cdot Y}\int_V u_L(\mathbf{x})d\mathbf{x}.$$

The LAI is the key variable in most ecosystem productivity models, and in global models of climate, hydrology, biogeochemistry and ecology that attempt to describe the exchange of fluxes of energy and mass momentum between the surface and the atmosphere.

3. Eigenvalues and eigenvectors of the radiative transfer equation

An eigenvalue of the radiative transfer equation is a number γ such that there exists a non-trivial function $e(\mathbf{x},\Omega)$ that satisfies $\gamma Le=S_\lambda e$ and zero boundary condition ($\rho_\lambda=0$ and $q_\lambda=0$). For the adjoint radiative transfer problem [11,13], an eigenvector $e^*(\mathbf{x},\Omega)$ corresponding to the eigenvalue γ satisfies $\gamma ULUe^*=S_\lambda e^*$ and zero boundary condition $e^*(\mathbf{x}_B,\Omega)=0$ for outgoing directions, $\mathbf{n}_B\cdot\Omega>0$. Here U is a linear operator that transforms functions $f(\mathbf{x},\Omega)$ into $f(\mathbf{x},-\Omega)$. Obviously, $U=U^{-1}$ and $US_\lambda U=S_\lambda$. It follows from these relationships that the eigenvectors $e(\mathbf{x},\Omega)$ and $e^*(\mathbf{x},\Omega)$ are related as $e^*=Ue$. It should be emphasized that the definition of the eigenvector incorporates both the forward and adjoint radiative transfer equations.

Vladimirov [11] formulated the eigenvalue/eigenvector problem in functional spaces D_θ and H_θ, $1\le\theta\le\infty$. The former specifies the domain of the operator L while the latter defines its range. The space D_θ consists of absolutely continuous functions $\varphi(\mathbf{x},\Omega)$ which satisfy the zero boundary condition ($\varphi(\mathbf{x}_B,\Omega)=0$, $\mathbf{n}_B\cdot\Omega<0$, $\mathbf{x}_B\in\delta V$) and $\|L\varphi\|_\theta<\infty$. Here $\|\cdot\|_\theta$ is the norm in the space H_θ defined as[1]

$$\|v\|_\theta=\left[\int_{V\times4\pi}\sigma(\mathbf{x},\Omega)|v(\mathbf{x},\Omega)|^\theta d\mathbf{x}d\Omega\right]^{1/\theta},\ \theta<\infty,$$

$$\|v\|_\infty=\sup_{V\times4\pi}\mathrm{vrai}\ |v(\mathbf{x},\Omega)|,\quad \theta=\infty.$$

The space D_θ is a dense subset of H_θ, $1\le\theta\le\infty$, and $D_\theta\subset D_q$ if $\theta>q$. The set $\{\gamma_k,\ e_k\}$ of eigenvalues, γ_k, and eigenvectors, $e_k(\mathbf{x},\Omega)$, is a discrete set and do not depend on θ, i.e., on functional spaces D_θ and H_θ in which the problem was formulated. The eigenvectors and their adjoints belong to the space D_∞ and are mutually orthogonal with respect to the operator S_λ, i.e., $(S_\lambda e_k,e_m^*)=\delta_{km}$. Here (. , .) denotes the scalar product of functions $f\in H_\theta$ and $f^*\in H_\theta^*=H_{\theta^*}$, $1/\theta+1/\theta^*=1$,

$$(f,f^*)=\int_{V\times4\pi}\sigma(\mathbf{x},\Omega)f(\mathbf{x},\Omega)f^*(\mathbf{x},\Omega)d\mathbf{x}d\Omega.$$

It follows from the definition of the eigenvector and orthogonality that $\gamma_k(Le_k,e_m^*)=\gamma_k\delta_{km}$. The radiative transfer equation has a positive eigenvalue, γ_0, that corresponds to a positive eigenvector, $e_0(\mathbf{x},\Omega)$. The eigenvalue γ_0 is greater than the absolute magnitudes of the remaining eigenvalues, i.e., $|\gamma_k|\le\gamma_0$. If $S_\lambda=\omega(\lambda)S_0$ (as assumed in Section 2), the eigenvectors do not depend on wavelength. The corresponding eigenvalues can be expressed as $\gamma_k=\omega(\lambda)p_k$ where p_k satisfies $p_kLe_k=S_0e_k$. Mathematical details of the above theory can be found in [11].

It should be noted that there is another formulation of the eigenvalues and eigenvectors in linear transport theory proposed by Case and Zweifel [15]. Their approach is similar to that used in the theory of ordinary differential equations, i.e., solutions of the homogeneous problem ($\rho_\lambda=0$ and $q_\lambda=0$) are represented as the product of an exponential function of spatial variable and corresponding eigenfunction which depends on angular variable. Unlike the definition given above, the Case and Zweifel formulation results in both discrete and continuum of eigenvalues. The eigenfunctions corresponding to the continuum of the eigenvalues are Schwartz distributions and, consequently, cannot be described in terms of the functional spaces D_θ and H_θ. Here, formulations of Vladimirov [11] and techniques of Knyazikhin et al. [4] are adopted.

4. Expansion in eigenvectors

Let $u_\lambda=dI_\lambda/d\lambda$. Differentiating Eqs. (1) and (2) with respect to wavelength, we get

$$Lu_\lambda=\frac{d}{d\lambda}S_\lambda I_\lambda=S_\lambda u+S'_\lambda I_\lambda \tag{3}$$

with zero boundary condition. Under our assumption regarding the scattering operator (Section 2), $S'_\lambda=\omega'(\lambda)S_0$. Thus, the derivative of I_λ with respect to the wavelength λ satisfies the radiative transfer equation with zero boundary condition ($u_\lambda\in D_\theta$) and an internal source given by $S'_\lambda I_\lambda$.

We expand the scattering term $S_\lambda I_\lambda$ in eigenvectors,

$$S_\lambda I_\lambda(\mathbf{x},\Omega)=a_0(\lambda)S_\lambda e_0(\mathbf{x},\Omega)+\sum_{k=1}^{\infty}a_k(\lambda)S_\lambda e_k(\mathbf{x},\Omega),$$

$$a_k(\lambda)=(S_\lambda I_\lambda,e_k^*). \tag{4}$$

Here we separate the positive eigenvector $e_0(\mathbf{x},\Omega)$ corresponding to the maximum positive eigenvalue γ_0 into the first summand. Let $u_k=d(a_ke_k)/d\lambda$. We will show that

$$u_\lambda(\mathbf{x},\Omega)=u_0(\mathbf{x},\Omega)+\sum_{k=1}^{\infty}u_k(\mathbf{x},\Omega) \tag{5}$$

satisfies Eq. (3). Substituting Eqs. (4) and (5) into Eq. (3) results in

$$\sum_{k=0}^{\infty}Lu_k=\sum_{k=0}^{\infty}\frac{d}{d\lambda}\gamma_k(\lambda)a_k(\lambda)Le_k=\sum_{k=0}^{\infty}L[\gamma'_k(\lambda)a_k(\lambda)e_k+\gamma_k(\lambda)u_k(\lambda)]$$

[1] "sup vrai" means *bounds almost everywhere* its argument from above. For example, assume $u(x)=1$, if $x\neq0$, and ∞ otherwise. In this case, sup $u(x)$, used in the derivation of Eq. (9), is ∞ but sup vrai $u(x)=1$. Sometimes "true sup" or "essential sup" are used instead of "sup vrai".

It follows from this equation and orthogonality of the eigenvectors that

$$\frac{d[a_k(\lambda)e_k(\mathbf{x},\Omega)]}{d\lambda}=\frac{\gamma'_k(\lambda)}{1-\gamma_k(\lambda)}a_k(\lambda)e_k(\mathbf{x},\Omega).$$

Solving this ordinary differential equation results in

$$a_k(\lambda)=\frac{1-\gamma_k(\lambda_0)}{1-\gamma_k(\lambda)}a_k(\lambda_0). \tag{6}$$

Thus if the set of functions $\{S_0e_k\}$ is complete for functions of S_0H_p, the series (5) satisfies Eq. (3). It follows from Eq. (6) that if we know coefficients of the expansion (4) at a wavelength λ_0, we can find the coefficients for any other wavelength.

Given $S_\lambda I_\lambda$ solution of the radiative transfer equation is $I_\lambda=Q+L^{-1}S_\lambda I_\lambda$ where Q describes the distribution of photons from the wavelength independent boundary source $q_\lambda=q_0$ that have not undergone interactions within the domain V. Substituting expansion (4) into this equation one obtains an expansion of the solution in eigenvectors

$$I_\lambda(\mathbf{x},\Omega)=Q(\mathbf{x},\Omega)+\sum_{k=0}^{\infty}a_k(\lambda)\gamma_k(\lambda)e_k(\mathbf{x},\Omega). \tag{7}$$

This equation provides a basis for obtaining various forms of the energy conservation law. The norm, $\|I_\lambda\|_\theta$ of the solution of the radiative transfer equation is among its important components. Formally one can estimate $\|I_\lambda\|_\theta$ by direct integration of Eq. (7) over spatial and angular variables. Below we demonstrate an alternative technique, which complement the expansion of the solution in eigenvectors.

The three-dimensional radiative transfer equation (1) with purely absorbing boundaries ($\rho_\lambda=0$) can be transformed to the integral equation $I_\lambda=L^{-1}S_\lambda I_\lambda+Q$ [2,13]. The term $Q(x,\Omega)$ describes the distribution of photons from the wavelength independent boundary source $q_\lambda=q_0$ that have not undergone interactions within the domain V. It satisfies the equation $LQ=0$ and the boundary condition (2) with $\rho_\lambda=0$. The operator L and the boundary source do not depend on wavelength and thus Q is wavelength independent. The adjoint equation has the form $I^*_\lambda=US_\lambda L^{-1}UI^*_\lambda+Q^*$. Solutions of the integral radiative transfer equation and its adjoint counterpart are related as $(I_\lambda,Q^*)=(Q,I^*_\lambda)$ [13]. Note that L^{-1} represents the inverse of the operator L that maps the space D_θ into the space H_θ. Eigenvalues and eigenvectors of the operator $L^{-1}S_\lambda$ and its adjoint form $(L^{-1}S_\lambda)^*=US_\lambda L^{-1}U$ are $\{\gamma_k, e_k\}$ and $\{\gamma_k,Se^*_k\}$, respectively.

Obviously, $I^*_\lambda=(1-\gamma_k(\lambda))^{-1}S_0e^*_k$ satisfies the adjoint equation with $Q^*=S_0e^*_k$. Letting $S_0e^*_k$ in the relationship between solutions of the forward and adjoint radiative transfer, one arrives at

$$\begin{aligned}(I_\lambda,S_0e^*_k)&=(Q,I^*_k)=\frac{1}{1-\gamma_k(\lambda)}(Q,S_0e^*_k)\\&=\frac{1-\gamma_k(\lambda_0)}{1-\gamma_k(\lambda)}\frac{1}{1-\gamma_k(\lambda_0)}(Q,S_0e^*_k)\\&=\frac{1-\gamma_k(\lambda_0)}{1-\gamma_k(\lambda)}(Q,I^*_{\lambda_0})=\frac{1-\gamma_k(\lambda_0)}{1-\gamma_k(\lambda)}(I_{\lambda_0},S_0e^*_k).\end{aligned} \tag{8}$$

Thus given $(I_\lambda,S_0e^*_k)$ at wavelength λ_0, we can evaluate this function at any other wavelength. The term $(I_{\lambda_0},S_0e^*_k)$ on the right hand side of Eq. (8) depends on the incoming radiation while its factor is independent of illumination conditions and is a function of the intrinsic canopy properties. This relationship is similar to that given by Eq. (6).

The norm, $\|I_\lambda\|_1=(I_\lambda,1)$ of the solution of the radiative transfer equation is a very important component of the energy conservation law. The norm gives the mean number of photon interactions with phytoelements in the domain V. It can accurately be estimated from field measurements (Section 6). Given the number of interactions and the single scattering albedo, one can evaluate canopy absorption [2] and scattering [3]. A question then arises of how well $(I_\lambda,S_0e^*_0)$ approximates the norm $\|I_\lambda\|_1=(I_\lambda,1)$. The operator S_0 integrates the eigenfunction e^*_0, smoothing angular variation of the resulting function $S_0e^*_0$. In the case of an isotropic scattering for example $S_0e^*_0$ is independent of the angular variable and acts as a spatially varying isotropic source. Thus the proximity $(I_\lambda,S_0e^*_0)$ and $(I_\lambda,1)$ depends on how the term $S_0e^*_0$ varies with the spatial variable. The following estimate gives a general idea of their closeness.

Let $T_0=L^{-1}S_0$ and $\eta=\sup\|T_0f\|_1/\|f\|_1$ where supremum is taken over all positive functions f from H_1. The norm $\|T_0f\|_1$ can vary with f significantly. However, it does not necessary involve large variation in the ratio $\|T_0f\|_1/\|f\|_1$. A theoretical explanation of this result can be found in the linear operator analysis [16] and, specifically, in its applications to radiative transfer theory [2,17–19]. The number η is an estimate of variation in $\|T_0f\|_1/\|f\|_1$ from above. It can be shown that $p\le\eta\le 1-\exp(-K)$ where p is the maximum positive eigenvalue of T_0 and the exponent K is a canopy structure dependent function [17]. Techniques for the estimation of the ratio $\|T_0f\|/\|f\|$ from above and from below and their relationship with the maximum eigenvalue p (recollision probability) can be found in [18].

Eq. (3) can be rearranged to an initial value problem for ordinary differential equation in functional spaces [16], i.e., $u_\lambda=\omega'(E-\omega T_0)^{-1}T_0I_\lambda$ with an initial value given by $I_\lambda\in H_1$ at $\lambda=\lambda_0$. Under the assumptions formulated in Section 2, the radiative transfer equation has a unique positive solution [11,12,15,17] and thus $(u_\lambda,1)=d(I_\lambda,1)/d\lambda=d\|I_\lambda\|_1/d\lambda$ and $((E-\omega T_0)^{-1}T_0I_\lambda,1)=\|(E-\omega T_0)^{-1}\,T_0I_\lambda\|_1$. We have

$$\begin{aligned}\frac{d\|I_\lambda\|_1}{\omega' d\lambda}&=\|(E-\omega T_0)^{-1}T_0I_\lambda\|_1\\&\le\|I_\lambda\|_1\sup_{f(\mathbf{x},\Omega)>0}\frac{\|(E-\omega T_0)^{-1}T_0f\|_1}{\|f\|_1}\le\frac{\eta}{1-\eta\omega(\lambda)}\|I_\lambda\|_1\end{aligned}$$

Solving this inequality for $\|I_\lambda\|_1$ yields

$$\|I_\lambda\|_1\le\frac{1-\omega(\lambda_0)\eta}{1-\omega(\lambda)\eta}\|I_{\lambda_0}\|_1. \tag{9}$$

Thus we have expressed the relationship between $\|I_\lambda\|_1$ and $\|I_{\lambda_0}\|_1$ in terms of the variation η. The norms depend on the full set of eigenvectors/values. If $\|T_0f\|_1/\|f\|_1$ does not vary significantly, i.e., $\|T_0f\|_1/\|f\|_1\approx const\approx\eta$, the norm $\|I_\lambda\|_1$ follows the spectral invariant relationship (9) similar to that given by Eq. (8). The term $S_0e_0^*$ in $(I_\lambda,S_0e_0^*)$ can be replaced with a constant function without violation of the spectral invariant relationship in this case. Our data analyses [6,20] and model calculations [21] suggest that $(I_\lambda,1)/(I_{\lambda 0},1)\approx(I_\lambda,S_0e_0^*)/(I_{\lambda_0},S_0e_0^*)$. These properties suggest a dominant role of the maximum eigenvalue in the energy conservation law for a canopy at any wavelength in the solar spectrum.

Relationships (8) for $k=0$ underlie the concept of canopy spectral invariants. Under our assumption regarding the scattering operator (Section 2) the ratio $p=\gamma_0/\omega(\lambda)$ is wavelength independent, coincides with the maximum positive eigenvalue of the radiative transfer equation in the vegetation canopy with perfectly reflecting phytoelements ($\omega(\lambda)=1$) and therefore satisfies $pLe_0=S_0e_0$. Solving this equation for p yields $p=L^{-1}S_0e_0/e_0$. The operator $L^{-1}S_0$ inputs the source e_0, simulates the scattering event (S_0) and the photon free path (L^{-1}) and outputs the distribution of photons just before their next interaction with phytoelements. The ratio therefore can be treated as the probability that a photon scattered from a phytoelement will interact within V again. We term this ratio, the recollision probability [3,6]. Under the conditions discussed above the recollision probability and single scattering albedo play a dominant role in the energy conservation law for a canopy at any wavelength in the solar spectrum.

5. Canopy spectral invariants: theory

Consider a domain V with non-reflecting boundary δV. Let t_0, zero order transmittance, be the portion of photons incident on the domain V that exit V without experiencing a collision. The interceptance, i_0, correspondingly denotes the portion of incoming photons that collide with phytoelements for the first time, and thus $t_0+i_0=1$. The zero order transmittance and interceptance do not depend on wavelength [3,6]. Portion, $a(\lambda,V)$, of intercepted photons will be absorbed within the domain V, while another portion, $s(\lambda,V)$, will be scattered out from V. The energy conservation law formulated for the domain V takes the following form [3]:

$$a(\lambda,V)+s(\lambda,V)+t_0=1.$$

Given the single scattering albedo $\omega(\lambda)$, the fraction of radiation absorbed by the domain V at the wavelength λ can be evaluated as $a(\lambda,V)=[1-\omega(\lambda)](I_\lambda,1)/F$, where F is the incident flux, which is assumed to be unity. Our data analyses [6,20], model calculations [21] and theoretical analyses (Section 4) suggest that

$$\frac{(I_\lambda,1)}{(I_{\lambda_0},1)}\approx\frac{(I_\lambda,S_0e_0^*)}{(I_{\lambda_0},S_0e_0^*)}. \tag{10}$$

It follows from Eqs. (8) and (10) that the absorptance can be approximated as

$$a(\lambda,V)=\frac{1-p\omega(\lambda_0)}{1-p\omega(\lambda)}\frac{1-\omega(\lambda)}{1-\omega(\lambda_0)}a(\lambda_0,V). \tag{11}$$

If $\omega(\lambda_0)=0$, the corresponding absorptance coincides with the interceptance, i.e., $a(\lambda_0,V)=i_0$. The energy conservation law can be rearranged to the form

$$\frac{1-\omega(\lambda)}{1-p\omega(\lambda)}i_0+W(\lambda,V)i_0=i_0. \tag{12}$$

Here $W(\lambda,V)=s(\lambda,V)/i_0$ is the single scattering albedo of the domain V defined as the probability that a photon intercepted by V will escape the domain V [3,9]. It follows from Eq. (12) that [3]

$$W(\lambda,V)=\omega(\lambda)\frac{1-p}{1-p\omega(\lambda)}. \tag{13}$$

Smolander and Stenberg [3] documented scaling properties of $W(\lambda,V)$. Consider a domain V that consists of objects (e.g., shoots in a coniferous forest V) of volume V_1 distributed within V in a certain fashion. We denote the single scattering albedo of V_1 by $\omega(\lambda)$. Scattering properties of the domain V and its constituent objects are related via Eq. (13). Let each object V_1 in turn consists of smaller objects, V_2 (e.g. needles in the shoot), and their scattering properties are given by $\omega(\lambda,V_2)$ (e.g., needle single scattering albedo). Eq. (13) can also be applied to the volume V_1, i.e.,

$$\omega(\lambda)=\omega(\lambda,V_2)\frac{1-p_{2,1}}{1-p_{2,1}\omega(\lambda,V_2)}. \tag{14}$$

The recollision probability $p_{2,1}$ refers to the volume V_1 and quantifies the event that a photon scattered by the object V_2 residing in V_1 (e.g., needle in the shoot) will interact within V_1 again (e.g., hit another needle within the same shoot). Substitution of Eq. (14) into Eq. (13) results in the same equation for $W(\lambda,V)$ with the only difference that $\omega(\lambda)$ is replaced with $\omega(\lambda,V_2)$ and p is replaced with a new recollision probability p_2 calculated as $p_2=p_{2,1}+(1-p_{2,1})p$. One can see that (i) the probability p_2 that a photon scattered by a volume V_2 (e.g., needle) will interact within the domain V again follows the Bayes' formula and (ii) a decrease in scale from V_1 (e.g., shoot) to V_2 (e.g., needle) is accompanied by an increase in the recollision probability from p to $p_{2,1}+(1-p_{2,1})p$. Schull et al. [22] applied this procedure for several nested sets of objects and found that the recollision probability increases with the number of nested hierarchical levels. They used this property to discriminate dominant forest type using hyperspectral surface reflectance. Lewis and Disney [23] found that Eqs. (13) and (14) are applicable to the leaf (V_1=leaf) and within leaf (V_2=a within-leaf scattering object) scales, implying that these equations provide a framework through which structural information can be maintained in a consistent manner across multiple scales from within-leaf to canopy level scattering. The recollision probability, therefore, is a scaling parameter that accounts for the cumulative effect of multi-level hierarchical structure in a vegetated pixel.

Let a parallel beam of unit intensity be incident on the upper boundary of a pixel V. Photons scattered by objects $V_1\subset V$ can escape the pixel V in a given direction Ω. Their angular distribution is given by the directional escape probability $\rho(\Omega)$ [6]. Given the single scattering albedo, $\omega(\lambda)$, the recollision, p, and escape, ρ, probabilities at the scale V_1, as well as the interceptance, i_0, the bidirectional reflectance factor (Section 2) of the pixel V bounded by a non-reflecting surface δV can be approximated as

$$BRF(\lambda,\Omega)=\frac{\rho(\Omega)i_0\omega(\lambda)}{1-\omega(\lambda)p}. \quad (15)$$

This quantity is a standard product of MODIS and MISR instruments of the EOS Terra mission [24].

Eq. (11) for $\omega(\lambda_0)$=0 and (15) can be rearranged to a form which we use to obtain the spectral invariants p and $R(\Omega)=\rho(\Omega)i_0$ from satellite and ground based measurements, namely,

$$i(\lambda)=pi(\lambda)\omega(\lambda)+i_0,\quad \frac{BRF(\lambda,\Omega)}{\omega(\lambda)}=pBRF(\lambda,\Omega)+R(\Omega). \quad (16)$$

Here $i(\lambda)=a(\lambda,V)/[1-\omega(\lambda)]=\|I_\lambda\|_1$ is the interaction coefficient. For a pixel bounded by a non-reflected surface, this variable is the mean number of photon interactions with objects V_1 at wavelength λ. By plotting $i(\lambda)$ versus $i(\lambda)\omega(\lambda)$, a linear relationship is obtained, where the slope and intercept give the recollision probability and the canopy interceptance. Similarly, the slope and intercept of the BRF/ω versus BRF line are the recollision, p, probability and escape factor, $R(\Omega)=\rho(\Omega)i_0$, respectively. Thus, simple algebraic combinations of leaf and canopy spectral reflectance become wavelength independent and determine two canopy structure specific variables – the recollision and escape probabilities. It should be noted that Eqs. (16) are directly applicable only to dense canopies or canopies with a sufficiently dark background. In general case the use of the spectral invariant relationships should follow after the removal of the background reflectance from the BRF of canopy-surface system [4,5].

6. Canopy spectral invariants: observations

Fig. 1 demonstrates the first relationships in (16). In this example V represents a 50×50 m^2 plot composed of Norway spruce located at Flakaliden Research Area (64°14′ N; 19°46′ E) operated by the Swedish University of Agricultural Sciences [6]. The LAI, forest cover and tree density are 4.4, 0.8 and 1800 stems/ha, respectively. Simultaneous measurements of up- and downward radiation fluxes for a spectral range of 400–1000 nm with a 1.6 nm spectral resolution were taken from above and below the canopy using two spectroradiometers. A helicopter was used to take measurements above the canopy. These data were used to estimate canopy spectral absorptance $a(\lambda,V)$ [6]. Samples of spruce needles were collected from several locations and their optical properties were measured under laboratory conditions. From these data the mean single scattering albedo $\omega(\lambda,V_2)$ at the needle scale (V_2=needle) was obtained by averaging measured spectra [6]. By plotting $i(\lambda)$ versus $i(\lambda)\omega(\lambda)$, a linear relationship is obtained. This result supports the validity of the assumption (10).

Fig. 2 demonstrates the second relationship in (16). By plotting values of the ratio BRF/ω versus BRF for a vegetated pixel, a linear relationship is obtained, where the slope and intercept give the recollision probability and directional escape factor, respectively. The wavelength independent recollision probability is the probability that a photon scattered from a phytoelement will interact within the canopy again and is related to the maximum eigenvalue of the radiative transfer equation (Section 4). This parameter accounts for a cumulative effect of the canopy structure over a wide range of scales (Section 5). For example, if a vegetation canopy is treated as a big leaf, i.e., no structure and LAI is 1, the recollision probability is zero because a photon reflected or transmitted by one "big" leaf will not encounter another leaf. If one cuts the leaf into "small pieces" and uniformly distributes the pieces in a canopy layer (the structure has changed with LAI unaltered), the recollision probability changes its value from zero to about 0.3 [3]. At a given LAI, the recollision probability increases with the number of hierarchical levels present in the landscape (e.g., the clumping of needles into shoots, shoots and leaves into crowns, etc., Section 5). The recollision probability combined with the LAI has the potential to discriminate between broadleaf and coniferous canopies as illustrated in Fig. 3 [25].

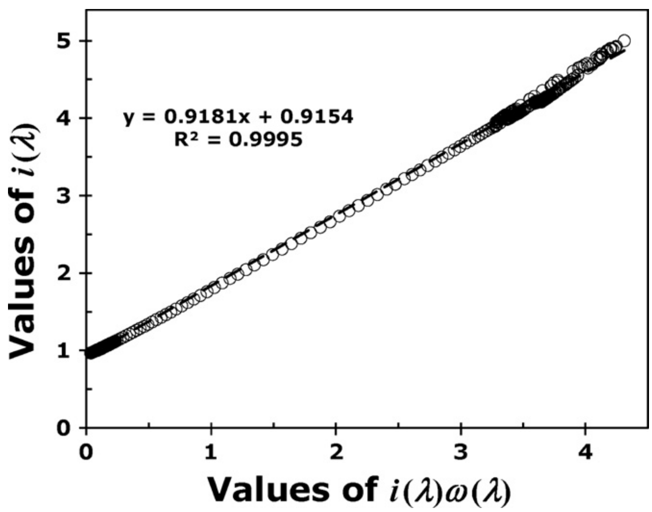

Fig. 1. Linear relationship between the interaction coefficient $i(\lambda)$ and $i(\lambda)\omega(\lambda)$ derived from field data supports the validity of the assumption (10).

Please cite this article as: Knyazikhin Y, et al. Canopy spectral invariants. Part 1: A new concept in remote sensing of vegetation. JQSRT (2010), doi:10.1016/j.jqsrt.2010.06.014

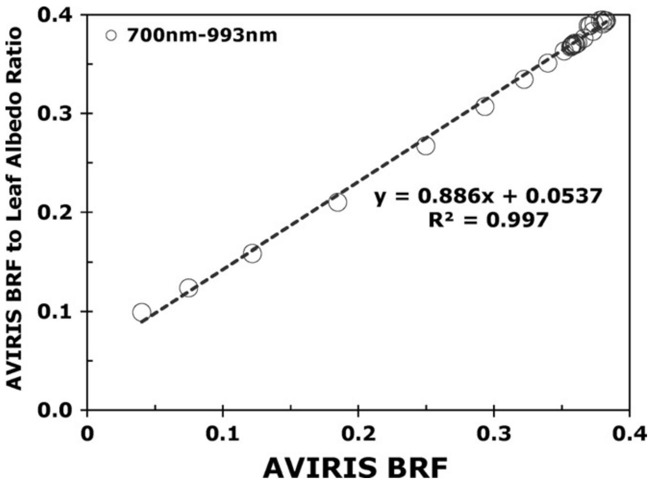

Fig. 2. By plotting values of the canopy reflectance to leaf albedo ratio, $BRF_\lambda/\omega_\lambda$, versus reflectance values, BRF_λ, for a vegetated pixel, a linear relationship is obtained, where the slope and intercept give the *recollision* probability and *escape* factor, respectively. The reflectance spectrum was obtained from Airborne Visible/Infrared Imaging Spectrometer (AVIRIS) data acquired over Bartlett Experimental Forest, New Hampshire, in the nadir direction. The AVIRIS sensor provides calibrated images of the up-welling spectral radiance in 224 contiguous spectral channels with wavelengths from 400 to 2500 nanometers at a spatial resolution of 3.3 m [WWW1[30]]. Note that a reference leaf albedo is used in this example. For more details the reader is referred to our companion paper [22].

The p versus LAI relationships shown in Fig. 3 were derived from canopy transmittances measured by LAI-2000 Canopy Analyzer (Li-Cor Inc.) using methodology proposed by Stenberg [26]. The LAI-2000 instrument's optical sensor consists of five detectors arranged in concentric rings measuring radiation between 320 and 490 nm. In this blue portion of the solar spectrum, foliage typically reflects and transmits relatively little radiation, i.e., $\omega(\lambda)\approx 0$. The measurements are typically taken shortly before sunset, or during overcast days when the forest is illuminated only by diffuse light. LAI-2000 readings, therefore, provide an accurate estimate of uncollided downward radiation Q in Eq. (8) below the vegetation canopy in five directions. In [26], the derivation of the p-LAI equation begins with the evaluation of the fraction of photons that will escape the canopy given that the photons are uniformly distributed on the canopy leaf area. Such an escape process can be described by the adjoint radiative transfer equation with $Q^*=(2\pi)^{-1}$. The probability, $1-p$, that a photon will escape the vegetation canopy as a result of one interaction can be approximated as $(Q,1)/((2\pi)^{-1},I^*_\lambda)$ when ω_λ approaches unity. The numerator accounts for photons from the isotropic boundary source intercepted by leaves. The intercepted photons are given by $1-t_0$ where the zero order transmittance t_0 can directly be obtained from LAI-2000 data. The denominator is the number of photon interactions with leaves before exiting the canopy given that photons before and after the first interaction are uniformly distributed on the canopy leaf area and the outgoing radiation coincides with the incident flux. Neglecting multiple interactions, this term gives LAI. At high LAI values however the photon multiple interactions may not by negligible and thus the use of Stenberg's equation [26] can lead to an overestimation of the recollision probability.

A strong correlation between canopy height and multi-angle spectral canopy reflectance has recently been documented [27,28]. Schull et al. [21] found that the directional escape factor (intercept in Fig. 2) is the variable that imbues the sensitivity of multi-angle spectral data to canopy height. The following analyses of Airborne Multi-Angle Imaging Spectrometer (AirMISR) [WWW2 [31]] and airborne Laser Vegetation Imaging Sensor (LVIS) [WWW3 [32]] data acquired during a NASA Terrestrial Ecology Program aircraft campaign over the Howland Forest (45.2 N, 68.74 W), Main, Harvard Forest (42.54 N, 72.17 W), Massachusetts, and Bartlett Experimental Forest (44.06 N, 71.29 W), New Hampshire, were performed to gain insight into the observed correlation. A random subset (training set) from 1/3 of the AirMISR-LVIS dataset was created to derive two multivariate linear regression models for estimating LVIS canopy height measures. The independent variables for the first model were AirMISR reflectances for 4 spectral bands at 7 view directions, totaling 28 variables. To obtain the second model, the escape factor at 7 AirMISR view angles using Eq. (15) was retrieved first and then used the obtained values as the 7 independent variables in the model. The models were then used to predict LVIS height measure from the AirMISR data and the escape factor in the remaining 2/3 of pixels (testing set). The correlation coefficients calculated using values of predicted and actual LVIS heights were employed as a measure of the information about canopy structure that AirMISR data and escape factor convey. Fig. 4 shows the correlation coefficients for AirMISR predicted LVIS height estimates versus correlations for escape probability predicted LVIS heights for three sites at two different observation geometries (principal and cross planes) and for ten combinations of training and testing sets. A detailed analysis of this plot can be found in [21]. Overall, the

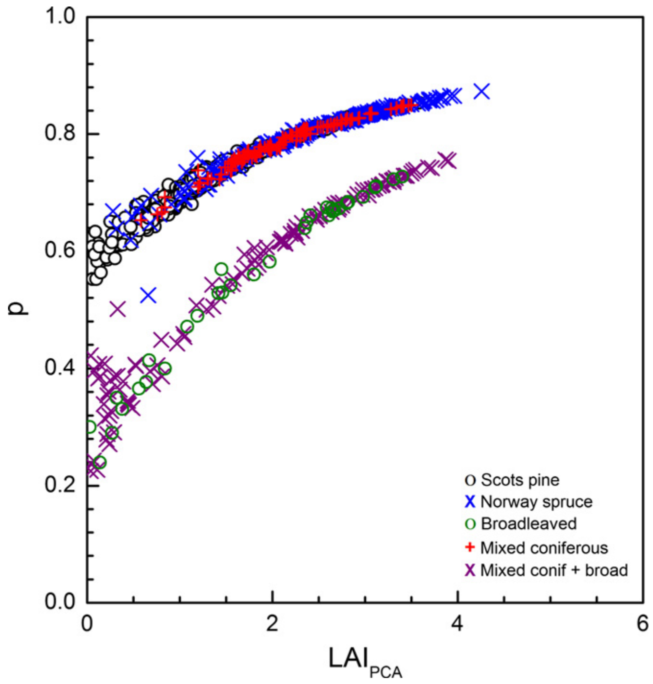

Fig. 3. The relationship between photon recollision probability and leaf area index for needle leaf and broadleaf forests (*From* [25]). Values of the recollision probability were derived from LAI-2000 data acquired over 1032 coniferous and broadleaved forest plots in Finland using methodology proposed by Stenberg [26].

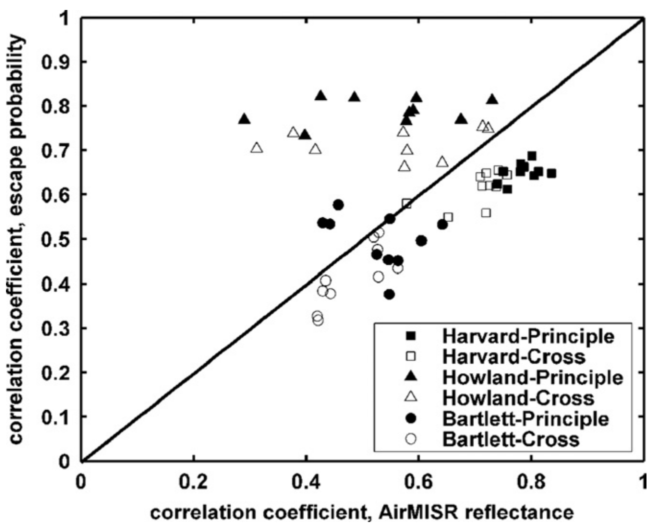

Fig. 4. Correlation coefficients for escape factor predicted heights versus correlations for AirMISR predicted heights for three sites at two different observation geometries (Principle and Cross planes) and ten combinations of training and testing sets. From [21].

wavelength independent escape factor and multi-angle spectral data tend to provide a comparable amount of information about the LVIS height measure. Disney et al. [29] documented the sensitivity of the escape factor and recollision probabilities to the stand age. Schull et al. [22] suggest that the location of points on the $|\log(1-p)|$ versus $|\log R/(1-p)|$ plane is determined by canopy structure at both the macro and micro scales and can be used to discriminate dominant forest type based on number of nested hierarchical levels present in the pixel, crown geometry, ground cover, within-crown foliage density and portion of sunlit and shadow leaves.

Recall that the spectrally invariant behavior is valid for a vegetation canopy bounded from below by a non-reflecting surface. Examples presented here are either for dense forests or forest patches with a sufficiently dark background. In general, the use of the spectral invariant relationships should follow after the removal of the background reflectance from the BRF of canopy-surface system [4,5].

7. Conclusions

The wavelength independent canopy interceptance, recollision and directional escape probabilities specify an accurate relationship between the spectral response of a vegetation canopy with non-reflecting background to incident radiation at the leaf and canopy scales. The recollision probability is the probability that a photon scattered from a phytoelement will interact within the canopy again and is equal to the maximum eigenvalue of the radiative transfer equation. The directional escape probability is the probability that a scattered photon will escape the vegetation in a given direction. This result was obtained by the expansion of the solution of 3D radiative transfer equation in eigenvectors. The independency of the interaction cross-section on wavelength was critical to relate canopy absorptive and reflective properties to the maximum eigenvalue. The canopy spectral invariants can be considered fundamental descriptors of the impact of canopy structure on canopy scattering where the scattering objects are large compared with the wavelength of radiation.

Acknowledgments

This research was funded by the Jet Propulsion Laboratory, California Institute of Technology under MISR contract 1259071, by the National Aeronautics and Space Administration (NASA) under Grants NNX09AI30G, NNX08AE81G, NNX08AL55G, and by NASA Headquarters under the NASA Earth and Space Science Fellowship Program under Grant NNX07AO41H.

References

[1] Ross J, The radiation regime and architecture of plant stands. Norwell, MA: Dr. W. Junk; 1981. 391 p.

[2] Knyazikhin Y, Marshak A, Myneni RB. Three-dimensional radiative transfer in vegetation canopies and cloud-vegetation interaction. In: Marshak A, Davis AB, editors. Three dimensional radiative transfer in the cloudy atmosphere. Berlin: Springer-Verlag; 2005. p. 617–52.

[3] Smolander S, Stenberg P. Simple parameterizations of the radiation budget of uniform broadleaved and coniferous canopies. Remote Sens Environ 2005;94:355–63.

[4] Knyazikhin Y, Martonchik JV, Myneni RB, Diner DJ. Running SW. Synergistic algorithm for estimating vegetation canopy leaf area index and fraction of absorbed photosynthetically active radiation from MODIS and MISR data. J Geophys Res 1998;103:32257–74.

[5] Knyazikhin Y, Martonchik JV, Diner DJ, Myneni RB, Verstraete MM, Pinty B, et al. Estimation of vegetation canopy leaf area index and fraction of absorbed photosynthetically active radiation from atmosphere corrected MISR data. J Geophys Res 1998;103(D24): 32239–56.

[6] Huang D, Knyazikhin Y, Dickinson RE, Rautiainen M, Stenberg P, Disney M, et al. Canopy spectral invariants for remote sensing and model applications. Remote Sens Environ 2007;106:106–22.

[7] Dickinson RE, Zhou L, Tian Y, Liu Q, Lavergne T, Pinty B, et al. 3-dimentional analytic model for the scattering of a spherical bush. J Geophys Res 2008;113:D20113.

[8] Dickenson RE. Determination of the multi-scattered solar radiation from a leaf canopy for use in climate models. J Comput Phys 2008;227:3667–77.

[9] Ganguly S, Schull MA, Samanta A, Shabanov NV, Milesi C, Nemani RR, et al. Generating vegetation leaf area index earth system data record from multiple sensors. Part 1: Theory. Remote Sens Environ 2008;112:4333–43.

[10] Ganguly S, Samanta A, Schull MA, Shabanov NV, Milesi C, Nemani RR, et al. Generating vegetation leaf area index earth system data record from multiple sensors. Part 2: Implementation, Analysis and Validation. Remote Sens Environ 2008;112:4318–32.

[11] Vladimirov VS. Mathematical problems in the one-velocity theory of particle transport. Tech Rep AECL-1661, Ontario: At. Energy of Can. Ltd., Chalk River; 1963. 302 p.

[12] Germogenova TA. In: The local properties of the solution of the transport equation. Moscow: Nauka; 1986 272 p [in Russian].

[13] Davis AB, Knyazikhin Y. A primer in three-dimensional radiative transfer. In: Marshak A, Davis AB, editors. Three dimensional radiative transfer in the cloudy atmosphere. Berlin: Springer-Verlag; 2005. p. 153–242.

[14] Martonchik JV, Bruegge CJ, Strahler A. A review of reflectance nomenclature used in remote sensing. Remote Sens Rev 2000;19: 9–20.

[15] Case KM, Zweifel PF. In: Linear Transport Theory. Reading, MA. Addison-Wesley Publishing Company; 1967 342 p.

[16] Krein SG, editor. Functional analysis. Groningen: Wolters-Noordhoff; 1972.

[17] Knyazikhin Y, Marshak A. Fundamental equations of radiative transfer in leaf canopies and iterative methods for their solution. In: Myneni RB, Ross J, editors. Photon-vegetation interactions: applications in plant physiology and optical remote sensing. New York: Springer-Verlag; 1991. p. 9–43.

[18] Kaufmann RK, Zhou L, Knyazikhin Y, Shabanov NV, Myneni RB, Tucker CJ. Effect of orbital drift and sensor changes on the time series of AVHRR vegetation index data. IEEE Trans Geosci Remote Sens 2000;38:2584–97.

[19] Zhang Y, Shabanov N, Knyazikhin Y, Myneni RB. Assessing the information content of multiangle satellite data for mapping biomes. II. Theory. Remote Sens Environ 2002;80:435–46.

[20] Panferov O, Knyazikhin Y, Myneni RB, Szarzynski J, Engwald S, Schnitzler KG, et al. The role of canopy structure in the spectral variation of transmission and absorption of solar radiation in vegetation canopies. IEEE Trans Geosci Remote Sens 2001;39: 241–53.

[21] Schull MA, Ganguly S, Samanta A, Huang D, Shabanov NV, Jenkins J, et al. Physical interpretation of the correlation between multi-angle spectral data and canopy height. Geophys Res Lett 2008;34: L1845.

[22] Schull MA, Knyazikhin Y, Xu L, Samanta A, Ganguly S, Latorre Carmona P, et al. Canopy spectral invariants. Part 2: application to classification of forest types from hyperspectral data. J Quant Spectrosc Radiat Trans 2010, this issue, doi:10.1016/j.jqsrt.2010.06.004.

[23] Lewis P, Disney M. Spectral invariants and scattering across multiple scales from within-leaf to canopy. Remote Sens Environ 2007;109:196–206.

[24] Diner DJ, Braswell BH, Davies R, Gobron N, Hu J, Jin Y, et al. The value of multiangle measurements for retrieving structurally and radiatively consistent properties of clouds, aerosols, and surfaces. Remote Sens Environ 2005;97:495–518.

[25] Rautiainen M, Mõttus M, Stenberg P. On the relationship of canopy LAI and photon recollision probability in boreal forests. Remote Sens Environ 2008;113:458–61.

[26] Stenberg P. Simple analytical formula for calculating average photon recollision probability in vegetation canopies. Remote Sens Environ 2007;109:221–4.

[27] Kimes DS, Ranson KJ, Sun G, Blair JB. Predicting lidar measured forest vertical structure from multi-angle spectral data. Remote Sens Environ 2006;100:503–11.

[28] Heiskanen J. Tree cover and height estimation in the Fennoscandian tundra–taiga transition zone using multiangular MISR data. Remote Sens Environ 2006;103:97–114.

[29] Disney M, Lewis P, Quaife T, Nichol C. A spectral invariant approach to modeling canopy leaf scattering. In: Proceedings of the 9th ISPMSRS, Beijing, China, 17–19 October, Part 1, 2005. p. 318–20.

[30] WWW1: Airborne visible/infrared imaging spectrometer (AVIRIS) homepage. 〈http://aviris.jpl.nasa.gov〉.

[31] WWW2: AirMISR data and information, Atmospheric science data center. 〈http://eosweb.larc.nasa.gov/PRODOCS/airmisr/table_airmisr.html〉.

[32] WWW3: Laser vegetation imaging sensor (LVIS), NASA Goddard space flight center. 〈https://lvis.gsfc.nasa.gov〉.